

# UC Irvine

## UC Irvine Previously Published Works

### Title

Simultaneous assessment of human brain functional hemodynamics by magnetic resonance and near-infrared imaging

### Permalink

<https://escholarship.org/uc/item/3wq7s6hf>

### Authors

Toronov, Vladislav Y  
Webb, Andrew  
Choi, Jee H  
[et al.](#)

### Publication Date

2001-06-28

### DOI

10.1117/12.430911

### Copyright Information

This work is made available under the terms of a Creative Commons Attribution License, available at <https://creativecommons.org/licenses/by/4.0/>

Peer reviewed

# Simultaneous Assessment of Human Brain Functional Hemodynamics by Magnetic Resonance and Near-Infrared Imaging

Vladislav Toronov<sup>a</sup>, Andrew Webb<sup>a,b</sup>, Jee Hyun Choi<sup>c</sup>, Martin Wolf<sup>c</sup>, Enrico Gratton<sup>c</sup>

<sup>a</sup>Beckman Institute for Advanced Science and Technology, University of Illinois at Urbana-Champaign, 405 N.Mathews,Urbana. IL 61801

<sup>b</sup>Department of Electrical and Computer Engineering, University of Illinois at Urbana-Champaign

<sup>c</sup>Laboratory for Fluorescence Dynamics, Department of Physics, University of Illinois at Urbana-Champaign, 1110 West Green Street, Urbana, Illinois 61801

## ABSTRACT

Near-infrared spectroscopy is a relatively new imaging method, which can provide important information on concentrations of oxy- and deoxy-hemoglobin in cortical areas of the brain. We discuss the advantages of the integration of magnetic resonance and optical imaging techniques and present the results of our experimental study on the comparison of optical and fMRI signals obtained simultaneously on humans during functional activity and at rest. In all subjects we found a good collocation of the brain activity centers revealed by both methods. We also found a high temporal correlation between the BOLD signal (fMRI) and the deoxy-hemoglobin concentration (near-infrared spectroscopy) in the subjects who exhibited low fluctuations in superficial head tissues. The contamination of optical signals by superficial tissue layers urges applying algorithms of three-dimensional optical tomography.

Keywords: brain, near-infrared spectroscopy, fMRI

## INTRODUCTION

Functional magnetic resonance imaging (fMRI) is one of the most important techniques for brain function studies. It provides high spatial resolution at data acquisition rates of up to twenty images per second. The fundamental principle behind fMRI is the blood oxygenation level dependence (BOLD) of the MRI signal<sup>1</sup>. However, little information about the *absolute* changes in oxy- ( $O_2Hb$ ) and deoxy-hemoglobin ( $HHb$ ) concentrations can be obtained from BOLD signal. For cortical brain areas such information can be obtained using near-infrared (NIR) spectroscopy and imaging<sup>2,3</sup>. This relatively new method provides optical spectroscopic information about the concentrations of oxy- and deoxy-hemoglobin. Although the spatial resolution of NIR imaging is significantly limited by the nature of light propagation in tissue, potentially it can be developed to reach an acceptable level for practical applications at a significantly lower financial cost than fMRI.

Many measurements on humans and animals using near-infrared spectroscopy demonstrated its ability to assess brain activity<sup>4-10</sup>. However, there is a lack of direct comparison of near-infrared data with the ones obtained using other methods. In case of fMRI, such a comparison is important not only for validation and development of optical method, but also for better understanding the nature of fMRI signals. In this paper we discuss the advantages of the integration of magnetic resonance and optical imaging techniques and present the results of our experimental study on the comparison of near-infrared and fMRI signals obtained simultaneously on humans during functional activity and at rest.

## LIMITATIONS OF FUNCTIONAL MRI AND ADVANTAGES OF NEAR-INFRARED SPECTROSCOPY

The assessment of blood oxygenation changes by fMRI is based on the blood oxygenation level dependent (BOLD) effect<sup>1</sup>. To obtain a steady BOLD signal, a prolonged - typically between 30 and 60 sec - functional stimulation is used. The positive polarity of the stimulus-related signal component is commonly interpreted to reflect a decrease of  $[HHb]$  because of washout by an increased influx of fresh, oxygenated blood. Nevertheless, the exact physiological mechanisms behind the BOLD signal are still unresolved. Because the BOLD signal is sensitive to the ratio of deoxyhemoglobin to surrounding intravascular and extravascular water<sup>11</sup> a positive BOLD signal can be caused not only by deoxyhemoglobin washout from a given voxel but also by an increase in the water fraction in that voxel. A positive BOLD contrast can theoretically occur under several conditions: (1) if there is a decrease of deoxyhemoglobin caused by an increased influx of fresh oxygenated blood (depletion); (2) if the intravascular water fraction surrounding a given amount of deoxyhemoglobin increases, by an increase

in cerebral blood volume (CBV dilution); and (3) if both the intravascular amount of deoxyhemoglobin and CBV increase, but CBV increases more. The studies of functional brain hemodynamics in animals and humans by different methods show that both decrease and elevation of  $[HHb]$  in the activated area of the brain during stimulation are possible. Although the majority of studies favor the washout effect, in several studies the increase of  $[HHb]$  was observed<sup>4,5</sup>.

These limitations of fMRI have engendered an interest in integrating fMRI with optical methods<sup>6,7,9</sup>. The advantage of optical method is that it can provide spectroscopic information about the concentrations of both oxy- and deoxyhemoglobin in parenchymal tissue. Biological tissue is relatively transparent to light in the near-infrared band between 700 and 1000 nm (an optical window). Low-intensity near-infrared light entering tissue undergoes two major processes: absorption and scattering. Typically, an optical apparatus consists of a light source and a light detector, which receives light after it has been transmitted through the tissue. The light source is coupled to the tissue via optical fiber. Since light is highly scattered after entering tissue, another optical fiber bundle placed 2-5 cm away from the first one can collect light after it has passed through the tissue beneath the ends of the fibers (the optodes). Light that has traveled through the tissue is attenuated mainly due to absorption and scattering. This attenuation can be expressed mathematically in an empirical modified Lambert-Beer law<sup>2</sup>

$$\ln(I_0/I) = \mu \times d \times \sigma \quad (1)$$

where  $I_0$  and  $I$  are the input and output light intensity respectively,  $\mu$  is the medium absorption coefficient,  $d$  is the source-detector distance, and  $\sigma$  is the differential path length factor. The absorption coefficient  $\mu$  can be expressed as the product of the substance extinction coefficient  $\epsilon$  and the substance concentration  $c$ . A term  $\sigma > 1$  accounts for the longer effective pathlength of the light ray in the highly scattering medium than the geometric source-detector distance. A modified Lambert-Beer law indicates that the concentration and differential path length factor of a substance may be recovered from the light intensity measurements if, for example, the measurements are performed at several source-detector distances.  $O_2Hb$  and  $HHb$  have characteristic absorption spectra in visible and near-infrared bands. Therefore, based on light absorption measurements, concentration changes of these molecules can be measured. Light scattering occurs at the borders of media with different indices of refraction. Therefore, events occurring in neuronal membranes and volume changes of cellular compartments can influence light scattering<sup>10</sup>.

Substantial progress in the field of near-infrared spectroscopy and imaging of tissues was achieved when Chance, Patterson and Wilson showed that the optical parameters of turbid medium can be obtained from time-resolved measurements of short light pulses propagating in the medium<sup>12</sup>. During the same period, an equivalent concept utilizing intensity-modulated light sources was proposed by the group of E.Gratton<sup>13</sup>. Since this frequency-domain method has better sensitivity and is much faster than the time-domain method, the proposal of Gratton et al. was followed by many others<sup>14,15,16</sup>. A measurement with intensity modulated light yields three independent quantities: intensity (DC), modulation amplitude (AC) and phase. For a highly scattering homogeneous medium from any combination of two of them one can obtain the reduced scattering and absorption coefficients.

A number of theoretical studies attempted to investigate the spatial sensitivity of NIR imaging using computer simulation of light propagation in models of the head<sup>17,18</sup>. These studies showed that when the optodes are placed on the scalp surface, a NIR device can pick up changes in hemoglobin concentration on the cortical surface. The signal is limited to changes in hemodynamics occurring in the top 2-3 mm of the cortex. The area of the brain surface is approximately as wide as the optode spacing and extends laterally 1 cm either side, in a direction perpendicular to the optode position. The frequency-domain method is preferable over the continuous wave method because the spatial sensitivity of the phase is deeper than AC or DC profiles, although it is more difficult to provide a good signal-to-noise ratio in the phase than in AC and DC. However, it is commonly acknowledged that the results of these studies have limited practical implications for the reason that the optical properties of tissues in vivo are unknown. It is the advantage of simultaneous NIR and fMRI registration that the sensitivity of the light bundle to hemodynamic changes in the head can be directly assessed by comparison with the MR-BOLD signal.

### CORRELATION AND COLLOCATION OF SIMULTANEOUSLY ACQUIRED OPTICAL AND MR SIGNALS

We performed our measurements on six healthy right-handed male volunteers, 18 to 37 years old. Informed consent was obtained from all subjects. Each exercise run consisted of a 30-s pre-exercise epoch, ten 20-s stimulation epochs separated by ten 20-s control epochs, and a 50-s after-exercise epoch. During stimulation epochs subjects performed light palm squeezing

with the right hand with the frequency about 1.25 Hz. A computer program generating the commands for the subject and the scanner operator provided the synchronization of the exercise sequence with the MRI and NIRS recording.

Magnetic resonance imaging was performed using a 1.5 Tesla whole body MR scanner (Signa, General Electric Medical Systems, Milwaukee, WI) equipped with echospeed gradients and a standard circularly polarized birdcage head-coil. Sagittal T1-weighted localizer scans were used to determine the correct plane for the functional scans. Gradient-echo echo-planar images were acquired using a data matrix of 64 x 64 complex points, TR=640 ms, TE = 40 ms, FOV = 240 mm, slice thickness = 7 mm, no inter-slice gap, receiver bandwidth 62.5 kHz, and tip angle 90 degrees. The slices are parallel to the plane of three radiological markers on the optical probe. The middle slice (see Fig.1(a)) was set between the skull and the brain surface at C3 position. This slice was mostly filled with the cerebrospinal fluid (CSF), dura mater, arachnoidal tissue, pia mater, and a thin layer of the cortical tissue. Two deeper slices mostly contained the brain tissue, while two outer slices included the skull, the skin and the markers.

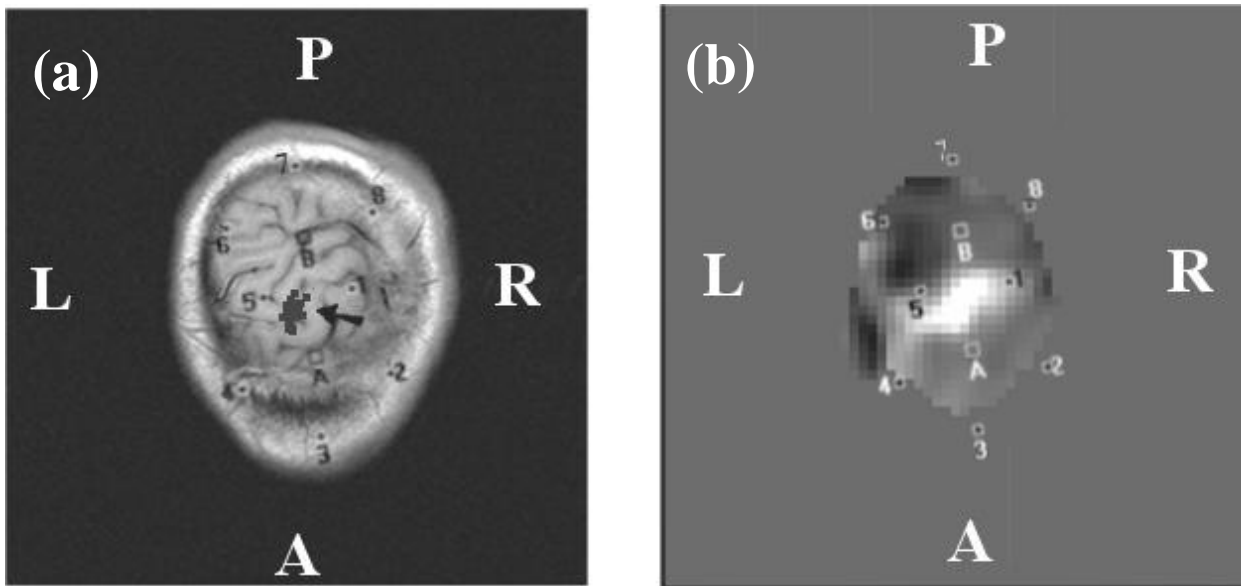


Fig.1. (a) Anatomical MR image of the middle slice in the motor cortex. (b) Statistical correlation image showing functional activation in the same slice. Sources are shown by dots numbered 1 through 8, and the detectors are indicated by squares with letters A and B. Letters “L”, “R”, “A”, and “P” indicate orientation and stand for “left”, “right”, “anterior”, and “posterior” respectively.

For NIRS measurements we used a two-wavelength (758 and 830 nm) frequency-domain (110 MHz modulation frequency) Oximeter (ISS, Champaign, IL), which had sixteen laser diodes (eight per each wavelength) and two photomultiplier tube detectors. At a wavelength of 758 nm light absorption by the deoxy-hemoglobin (HHb) substantially exceeded absorption by the oxy-hemoglobin (O<sub>2</sub>Hb), while at 830 nm the O<sub>2</sub>Hb absorption prevailed over the HHb absorption. The laser diodes operated in a sequential multiplexing mode with 10 ms “on” time per each diode. Light emitted by these laser diodes was guided to the tissue through 10-meter long multi-mode silica optical fibers. Two 10-m long glass fiber bundles collected the scattered light and brought it to the detectors. The paired (758 and 830 nm wavelength) source fibers were attached to the probe at 8 positions. Together with two detectors, they provided ten bi-wavelength source-detector channels with a source-detector distance of 3 cm. The optical probe covered an area 9 x 6 cm<sup>2</sup>. The probe was centered at the measured C3 position according to the International 10-20 System. Three multi-modality radiological markers (IZI Medical Products Corp, Baltimore, MD) were embedded into the optical probe to facilitate correct orientation of the MRI slices with respect to the probe and to enable recovery of the probe orientation for data analysis. In Fig. 1(a) the sources are shown by dots numbered 1 through 8, and the detectors are indicated by squares with letters A and B.

To convert optical intensity data into hemodynamic concentration changes, we used a model of light transport in strongly scattering medium based on the modified Lambert-Beer law (see Eq.(1)). Eq.(1) allows obtaining absorption coefficient at the given wavelength from intensity or modulation amplitude measurement. Changes of [O<sub>2</sub>Hb] and [HHb] corresponding to the changes in the absorption coefficients  $\Delta\mu_a^{\lambda_{1,2}}$  of the tissue at the wavelengths  $\lambda_1$  and  $\lambda_2$  can be obtained using the equations<sup>19</sup>

$$\Delta[\text{HbO}_2] = \frac{\Delta\mu_a^{\lambda_1} \epsilon_{\text{Hb}}^{\lambda_2} - \Delta\mu_a^{\lambda_2} \epsilon_{\text{Hb}}^{\lambda_1}}{\epsilon_{\text{HbO}_2}^{\lambda_1} \epsilon_{\text{Hb}}^{\lambda_2} - \epsilon_{\text{Hb}}^{\lambda_1} \epsilon_{\text{HbO}_2}^{\lambda_2}}, \quad (2)$$

$$\Delta[\text{Hb}] = \frac{\Delta\mu_a^{\lambda_2} \epsilon_{\text{HbO}_2}^{\lambda_1} - \Delta\mu_a^{\lambda_1} \epsilon_{\text{HbO}_2}^{\lambda_2}}{\epsilon_{\text{HbO}_2}^{\lambda_1} \epsilon_{\text{Hb}}^{\lambda_2} - \epsilon_{\text{Hb}}^{\lambda_1} \epsilon_{\text{HbO}_2}^{\lambda_2}}. \quad (3)$$

Here  $\epsilon_{\text{HHb}}^{\lambda_{1,2}}$  and  $\epsilon_{\text{O}_2\text{Hb}}^{\lambda_{1,2}}$  are the extinction coefficients of HHb and O<sub>2</sub>Hb, respectively, at wavelengths  $\lambda_1$  and  $\lambda_2$ .

Assuming synchronization between stimulation and hemoglobin response, we separate the functional response from background fluctuations by means of a folding average, i.e. the data corresponding to the same point on the stimulation/relaxation cycle is averaged over a number of cycles. The beginning of the time-locked period was chosen in the middle of the relaxation epoch.

The analysis of the fMRI data was performed using MEDx software (Sensor Systems, Inc). Prior to the statistical analysis, the data was subjected to the motion detection, spatial and temporal filtering, and global intensity normalization. Data with significant motion artifacts were discarded and measurements repeated. The resulting statistical images show the maps of coefficient  $r$  measuring correlation between voxel BOLD (EPI) intensity and a predictor function. As the reference function we used either the boxcar paradigm function with the “ON” and “OFF” durations equal to the stimulation and relaxation phases of the exercise, or the [HHb] signal obtained by NIRS taken with the opposite sign.

In all subjects the analysis of the BOLD signals during the motor task revealed a localised area under the optical probe where the signal was highly correlated with the paradigm boxcar function. It was an area in the primary motor cortex with the center close to the central sulcus (see Fig.1). White color of the highest intensity in Fig.1(b) corresponds to the correlation between the voxel BOLD signal and the paradigm boxcar function greater than 0.5. Using head landmarks for the C3 position, the center of the optical probe was placed very closely to the central sulcus so that light channels *A1*, *A5*, *B1*, and *B5* were above the activated area (compare Figs. 1 (a) and (b)). In all subjects the folding average analysis revealed the same type of [O<sub>2</sub>Hb] and [HHb] behavior for light channels situated above the major activated area as shown in Figure 2(a).

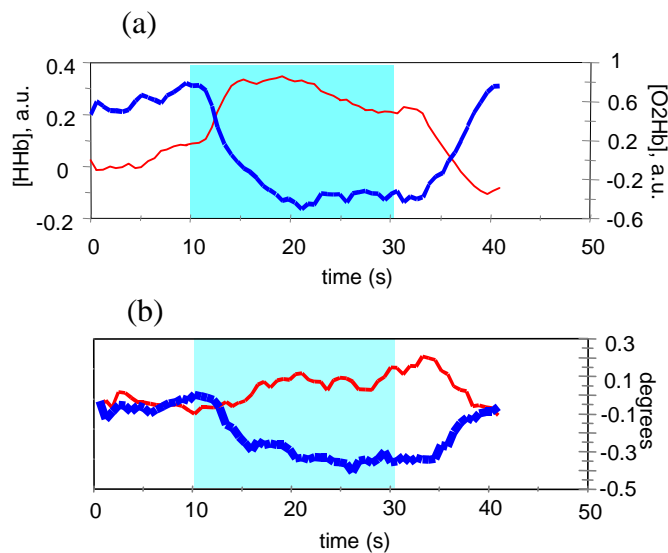


Fig. 2. Functional changes in optical signals. (a) Changes in [HHb] (thick line) and [O<sub>2</sub>Hb] (thin line). (b) Phase changes at 830 nm (thick line) and at 758 nm (thin line).

For the light channels situated above the activated area, the characteristic feature was a significant decrease of [HHb] during the stimulation, which was concurrent with a significant increase of the oxy-hemoglobin concentration. Typically rapid changes in [HHb] and [O<sub>2</sub>Hb] began 2-3 s after the stimulation onset and continued during next 7-15 s. Then [HHb] fluctuated near its low level for the rest of the stimulation epoch and the beginning of the resting epoch. After achieving its maximum, [O<sub>2</sub>Hb] either fluctuated at its high level or exhibited a slight decrease. A rapid recovery toward the baseline level begins 4-6 s after the onset of the rest epoch in both [HHb] and [O<sub>2</sub>Hb]. No significant decrease in the folding average [HHb] traces concurrent with the significant [O<sub>2</sub>Hb] increase was observed during stimulations in the light channels outside the activated area. Usually [HHb] in such channels fluctuated without correlation with the paradigm function. In some cases [O<sub>2</sub>Hb] increased, but without significant [HHb] change. In two subjects both [HHb] and [O<sub>2</sub>Hb] decreased in some channels during the stimulation indicating a decrease in blood volume in these non-activated regions.

To determine the location of the tissue contributing to the task-related changes in optical signals we performed a correlation analysis of the BOLD signals using the inverse NIRS [HHb] signals as the reference function. ([HHb] signal was taken with the opposite sign because an increase in BOLD signal should correspond to a decrease in [HHb].) In Fig. 1 (a) the arrow points at the clusters of voxels where  $z$  score for the correlation coefficient between BOLD signal and inverted [HHb] signal in channel A5 exceeded 10.0. One can see a good collocation of these clusters with the channel A5. Such a direct temporal correlation between optical and BOLD signals in cerebral and near-cerebral tissues was detected in three subjects. In other subjects no significant correlation between the intracranial BOLD signal and optically measured hemodynamic signals was detected, although the folding average [HHb] and [O<sub>2</sub>Hb] traces exhibited changes similar to the ones shown in Fig. 2(b). This low temporal correlation between the intracranial BOLD and optical signals was due to strong background hemodynamic fluctuations in optical signals contributed by the superficial tissues.

Having light intensity modulated at 110 MHz, we also analyzed the phase changes presumably caused by brain activity. Figure 2(b) shows the folding average phase traces for the light signals at 758 and 830 nm, corresponding to the hemodynamic changes shown in Fig.1. One can see that during the stimulation the phase of the 758-nm signal increases by 0.15 degree, and the phase of the 830-nm signal decreases by 0.3 degree. A similar behavior of the folding average traces of the phase in some of the channels close to the activated brain area was observed in four subjects. However, such a correspondence between phase and hemoglobin changes was not common. In many cases there was no apparent correlation between the phase and intensity behavior.

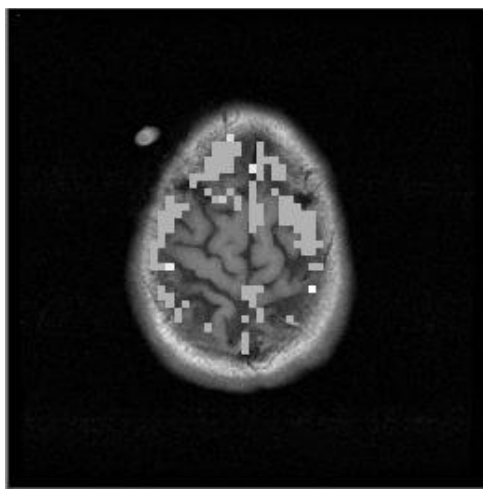


Fig.3. A map of correlation between the inversed [HHb] signal and the BOLD signal during rest. The marker near the left frontal area of the head slice indicates the position of the center of the optical source-detector pair.

We found significant temporal correlations between optically obtained hemodynamic signals and MR BOLD signals not only during the functional stimulations, but also at rest. Figure 3 shows areas of high correlation between the inversed [HHb] signal and the BOLD signal during rest. The optical signals were acquired from the left frontal area using the source-detector pair with separation of 35 mm. The areas of high correlation include not only regions immediately adjacent to the position of the optical probe, but also some remote areas. This was due to the correlation among spontaneous baseline hemodynamic fluctuations in different regions of the brain<sup>20</sup>.

## CONCLUSION

Although fMRI is a basic technique for imaging brain hemodynamics, its limitations urge developing another independent technique for measuring cerebral oxygenation. The NIR method uses a spectroscopic approach to this problem. Compared to other functional neuroimaging methods, NIR spectroscopy lacks spatial resolution and depth penetration, limiting most current studies to the cortical gray matter. On the other hand, NIR methods have some unique properties offering advantages over other methods, such as biochemical specificity by measuring concentrations of such substances as O<sub>2</sub>Hb, HHb and the cytochrome oxidase redox state. Optical methods have a good temporal resolution limited only by the signal to noise ratio. The cost of even highly sophisticated NIR imaging systems can be far less than the cost of other neuroimaging devices.

Analyzing near-infrared and BOLD signals acquired simultaneously under the motor stimulation conditions, we found a good collocation between the light channels with significant task-related folding average hemodynamic changes and the functionally activated area in the motor cortex in all subjects. A direct temporal correlation between NIRS and the intracranial BOLD signals was found in some subjects. These results confirm the intracranial origin of the NIRS signals obtained under the periodical stimulation conditions.

The lack of temporal correlation between the optical and fMRI signals in three subjects was due to the contamination of the optical signal by hemodynamic fluctuations in the superficial tissue layers. A significant sensitivity to the superficial changes is a drawback of the optical method. This problem can be resolved by using an algorithm of three-dimensional reconstruction of tissue optical properties from the data measured at many positions<sup>3</sup>. This method can be effectively enhanced by the frequency-domain approach<sup>13</sup>, i.e. using the phase of photon density waves irradiated by intensity-modulated light sources.

## REFERENCES

1. Thulborn K.R., Waterton J.C., Matthews P.M., Radda G.K., Oxygenation dependence of the transverse relaxation time of water protons in whole blood at high field, *Biochim Biophys Acta* **714**, 265-270 (1982)
2. Villringer A., Chance B., Non-invasive optical spectroscopy and imaging of human brain function, *Trends Neurosci.* **20**(10), 435-42 (1997)
3. Arridge S.R., Optical tomography in medical imaging, *Inverse Problems* **15**, R41-R93 (1999)
4. Kato T., Yamashita Y., Sugihara K., Furusho J., Tazaki I., Tanaka D., Maki A., Yamamoto T., Koizumi H., Ichikawa N., Iikura Y., Cerebral autonomic functional test using human functional near-infraredgraphy (FNIR), *NeuroImage* **9**, 221, (1999)
5. Hess, A., Stiller, D., Kaulisch, T., Heil, P., and Scheich, H., "New Insights into the Hemodynamic Blood Oxygenation Level Dependent Response through Combination of Functional Magnetic Resonance Imaging and Optical Recording in Gerbil Barrel Cortex", *J. of Neuroscience* **20**, 3328-3338 (2000)
6. Kleinschmidt A., H. Obrig, M. Requardt, K.D. Merboldt, U. Dirnagl, A. Villringer, J. Frahm, Simultaneous recording of cerebral blood oxygenation changes during human brain activation by magnetic resonance imaging and near-infrared spectroscopy, *J. Cereb. Blood. Flow Metab.* **16**(5), 817-826 (1996).
7. Gratton, G., Sarno A., Maclin E., Corballis, P.M., Fabianai, M., Toward noninvasive 3-D imaging of the time course of cortical activity: investigation of the depth of the event-related optical signal *Neuroimage* **11**, 491-504 (2000)
8. Toronov V., Franceschini M.A., Filiaci M., Fantini S., Wolf M., Michalos A., Gratton E., Near-infrared study of fluctuations in cerebral hemodynamics during rest and motor stimulation: temporal analysis and spatial mapping, *Med. Phys.* **27**(4), 801-15 (2000)
9. Toronov V., Webb A., Choi J.H., Wolf M., Michalos A., Gratton E., and Hueber D., Investigation of human brain hemodynamics by simultaneous near-infrared spectroscopy and functional magnetic resonance imaging, *Med. Phys. J.* (in press)
10. Gratton, G., Corballis, P.M., Cho, E., Fabianai, M., and Hood, D.C., Shades of gray matter: noninvasive optical images of human brain responses during visual stimulation, *Psychophysiology* **32**, 505-509 (1995)
11. Boxerman J.L., Bandettini P.A., Kwong K.K., Baker J.R., Davis T.L., Rosen B.R., Weisskoff R.M. The intravascular contribution to fMRI signal change: Monte Carlo modeling and diffusion-weighted studies in vivo. *Magn. Reson. Med.* **34**, 4-10 (1995)
12. Patterson M. S., Chance B., Wilson B.C., Time resolved reflectance and transmittance for the non-invasive measurement of tissue optical properties, *Appl. Opt.* **28**, 2231-2236 (1991)
13. Gratton E., Mantulin W.W., vande Ven M.J., Fishkin J.B., Maris, M.B., and B. Chance, The possibility of a near-infrared imaging system using frequency-domain methods, *Proc. Third Intl. Conf.: Peace through Mind/ Brain Science*, 183-189, Hamamatsu City, Japan (1990)

14. Boas D. A., O'Leary M. A., Chance B. , Scattering and wavelength transduction of diffuse photon density waves, *Phys. Rev. E* **47**, R2999-R3002 (1993)
15. Patterson M.S., Moulton J.,D., Wilson B.C., Berndt K., W., and Lakowicz J.R., Frequency-domain reflectance for the determination of the scattering and absorption properties of tissue, *Appl. Optics* **30**, 4474-4476 (1991)
16. Tromberg B., Svaasand L.O., Tsay T., Haskell R.C., Properties of photon density waves in multiple-scattering media, *Appl. Optics* **32**, 607-616 (1993)
17. Firbank M., Okada E., Delpy D.T., Investigation of the effect of discrete absorbers upon the measurement of blood volume with near-infrared spectroscopy, *Phys. Med. Biol.* **42**(3), 465-77 (1997)
18. Firbank M., Okada E., Delpy D.T., A theoretical study of the signal contribution of regions of the adult head to near-infrared spectroscopy studies of visual evoked responses, *Neuroimage*, **8**(1), 69-78 (1998)
19. Fantini S., Franceschini M. A., Maier J. S., Walker S. A., Barbieri B., and Gratton E., "Frequency-domain multichannel optical detector for noninvasive tissue spectroscopy and oximetry", *Optical Engineering* **34**, 32-42 (1995)
20. Biswal B., Yetkin F.Z., Haughton V.M., Hyde J.S., Functional connectivity in the motor cortex of resting human brain using echo-planar MRI, *Magn. Reson. Med.* **34**(4), 537-41, (1995)